Copyright © 2013 Tech Science Press CMES, vol.93, no.3, pp.167-186, 2013

Solutions of a Crack Interacting with Tri-Material Composite in Plane Elasticity

C.K. Chao[1], **A. Wikarta**[2]

Abstract: In this paper a crack interacting with tri-material composite under a remote uniform tensile load is solved in plane elasticity. An edge dislocation distribution along the prospective site of the crack together with the principle of superposition is used to model a crack. The resulting singular integral equation with logarithmic singular kernels for a line crack is then established. The singular integral equation is solved numerically by modeling a crack in place of several segments. Linear interpolation formulae with undetermined coefficients are applied to approximate the dislocation distribution along the elements, except at vicinity of crack tip where the dislocation distribution preserves a square-root singularity. Once the undetermined dislocation coefficients are solved, the mode-I and mode-II stress intensity factors can be obtained. Some numerical results are performed to show the effects of material property combinations and geometric parameters on the normalized mode-I and mode-II stress intensity factors.

Keywords: tri-material composite, arbitrarily oriented crack, logarithmic singular integral equation, stress intensity factors.

1 Introduction

A number of studies for solving crack problems have been investigated using Muskhelishvili complex potential in conjunction with singular integral equation approach. They include [Chao and Kao (1997); Chao and Young (1998)] for anti-plane problems, [Chen and Cheung (1990); Chen (1992); Chen and Chen (1997)] for in-plane problems, and [Chao and Shen (1995); Chao and Lee (1996)] for thermo-elasticity problems. In this approach, the fundamental solution of a point dislocation is required as a Green's function. By placing continuous distributions of dislocations along the prospective site of crack, the system of logarithmic singular integral equations is then formulated. All the above mentioned studies are

[1] National Taiwan University of Science and Technology (NTUST), Taipei, Taiwan, ROC.
[2] Institute of Technology Sepuluh Nopember,Kampus ITS Keputih, Indonesia

restricted to the problem containing cracks in a half-plane or two bonded half-plane media for which the solution of point dislocation can be expressed in closed form. The problem becomes more complicated when dealing with two or more interface boundaries, since the solution of point dislocation must be forced to satisfy both the boundary and interface continuity conditions. To overcome this difficulty, the technique of analytical continuation that is alternately applied across two different interfaces in order to derive the point dislocation solution in a series form [Choi and Earmme (2002); Chao and Chen (2004)] has been treated to solve such problem. Recently, a series form solution of dislocation has been used to simulate a crack interacting with multilayer media for anti-plane elasticity problems [Chao, Wikarta, and Korsunsky (2010); Chao and Wikarta (2012)]. This method obviously provides a reliable result making the series solution rapidly convergent. Another merit is that the solutions remain valid regardless of the shape and number of medium such as elliptically layered media and eccentrically coated circular inclusion.

In this present study, the interaction between a crack and a tri-material under remote uniform tensile load for in-plane elasticity is considered. Since our solution is expressed in terms of any homogeneous solution, the present methodology can be also applied to the problem subjected to a body force. The study can be achieved by determination of the stress intensity factors that allow the characterization of interaction from the point of view of linear elastic fracture mechanics. The solution procedures of this study are as follows. An edge dislocation distribution along the prospective site of the crack together with the principle of superposition is used to model a crack. The resulting singular integral equation with logarithmic singular kernels for a line crack is then established. The singular integral equation is solved numerically by modeling a crack in place of several segments. Linear interpolation formulae with undetermined coefficients are applied to approximate the dislocation distribution along the elements, except at vicinity of crack tip where the dislocation distribution preserves a square-root singularity. Once the undetermined dislocation coefficients are solved, the mode-I and mode-II stress intensity factors can be obtained.

The layout of the present paper is as follows. The problem statement and series form solutions for the complex potentials function are given in Section 2. The integral equations with logarithmic singular kernels for a line crack are established in Section 3. Some numerical examples are solved in Section 4. Finally, Section 5 concludes the article.

2 Problem formulation and solution of edge dislocation

Consider a tri-material occupying regions S_1: $y \leq 0$, S_2: $0 \leq y \leq t$; S_3: $y \geq t$, respectively, which are perfectly bonded along two parallel interfaces $L : y = 0$ and

$L*$: $y = t$as shown on Fig. 1. Let the tri-material contain a crack with length $2a$ located in region S_1 or region S_2 with distance h from interface L and subjected to a remote uniform tensile σ_x. Note that the loading condition shown in Fig. 1 is designed to satisfy continuity of strain across the interface such that perfectly bonded conditions between two regions are ensured.

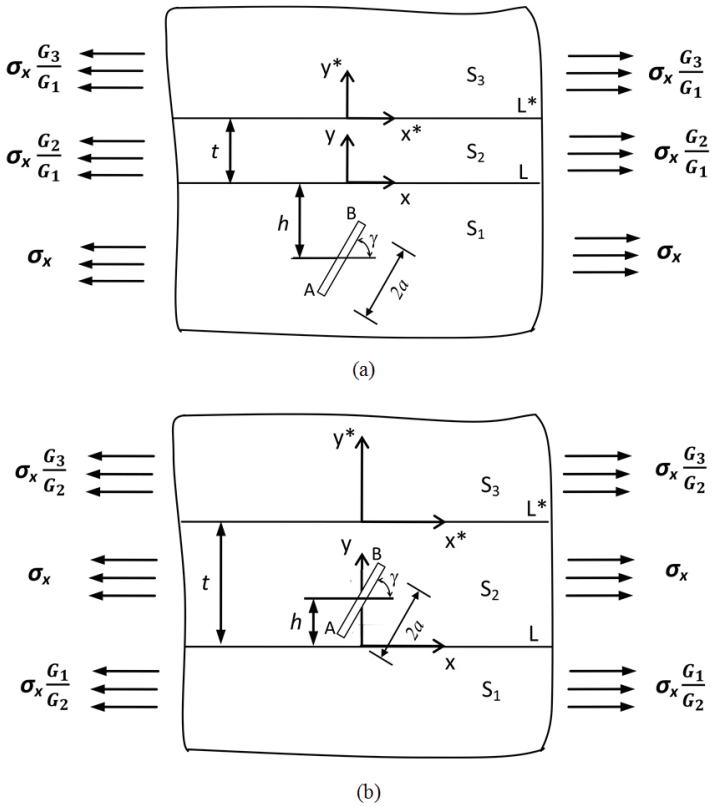

Figure 1: A tri-material composite with (a) crack located in region S_1 and (b) crack located in region S_2 subjected to uniform tensile load.

According to Muskhelishvili complex potential for in-plane elasticity, the component of displacement and resultant forces can be described by two complex functions $\varphi(z)$ and $\omega(z)$, each of which is analytic in its argument $z = x + i\,y$ for a two-dimensional problem, such as

$$2G(u+iv) = \kappa\phi(z) - \overline{\omega(z)} + (\bar{z}-z)\,\overline{\phi'(z)} \tag{1}$$

$$-Y + iX = \phi(z) + \overline{\omega(z)} + (z - \overline{z})\,\overline{\phi'(z)} \tag{2}$$

where $i^2 = -1$. In Eqs. (1) and (2), G is the shear modulus, κ = *3-4*υ for plane strain, and κ = *(3-*υ*)/(1+*υ*)* for plane stress, with υ being the Poisson's ratio. (') is designated as the derivative with respect to the associated argument, and a superimposed bar represents the complex conjugate.

In the problem associated with tri-material problems, the complex potential functions are found to depend on **non-dimensional parameters** as follows:

$$\Pi_{kj} = \frac{G_k - G_j}{G_k \kappa_j + G_j} \tag{3}$$

$$\Lambda_{kj} = \frac{G_k \kappa_j - G_j \kappa_k}{G_k + G_j \kappa_k} \tag{4}$$

where (*j, k = 1, 2, 3*)

The solution of an edge dislocation in a tri-material as shown in Fig. 2 is expressed in terms of the corresponding homogeneous problem subjected to the same loading. Based on analytical continuation theorem that is alternately applied across two different interfaces in complex plane, the series form solution has been provided by [Choi and Earmme (2002)].

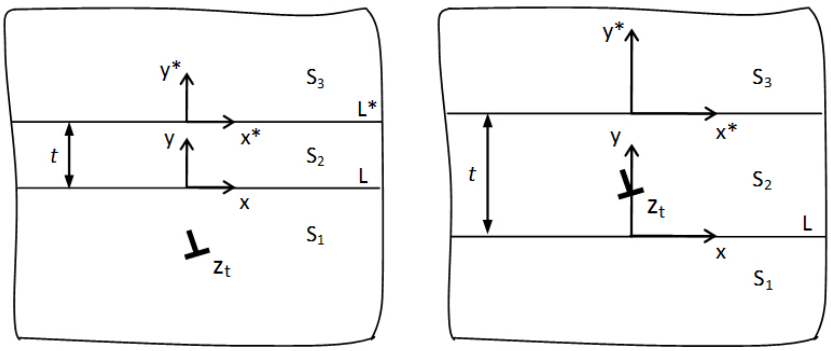

Figure 2: A tri-material composite with (a) edge dislocation located in region S_1 and (b) edge dislocation located in region S_2.

2.1 Edge dislocation in region S_1

The complete complex potential solution for an edge dislocation in region S_1 of the tri-material as shown in Fig. 2(a) is

$$\phi(z)=\begin{cases}(1+\Lambda_{32})\sum\limits_{n=1}^{\infty}\phi_n(z)\ z\in S_3\\ \sum\limits_{n=1}^{\infty}\phi_n(z)+\Lambda_{12}^{-1}\sum\limits_{n=1}^{\infty}\overline{\omega_{n+1}}(z)\ z\in S_2\\ \phi_0(z)+\Pi_{21}\overline{\omega_0}(z)+\left(1+\Lambda_{12}^{-1}\right)\sum\limits_{n=1}^{\infty}\overline{\omega_{n+1}}(z)\ z\in S_1\end{cases}\tag{5}$$

$$\omega(z)=\begin{cases}(1+\Pi_{32})\sum\limits_{n=1}^{\infty}\omega_n(z)+2it(\Lambda_{32}-\Pi_{32})\sum\limits_{n=1}^{\infty}\phi_n'(z)\ z\in S_3\\ \sum\limits_{n=1}^{\infty}\omega_n(z)+\Pi_{12}^{-1}\sum\limits_{n=1}^{\infty}\overline{\phi_{n+1}}(z)\ z\in S_2\\ \omega_0(z)+\Lambda_{21}\overline{\phi_0}(z)+\left(1+\Pi_{12}^{-1}\right)\sum\limits_{n=1}^{\infty}\overline{\phi_{n+1}}(z)\ z\in S_1\end{cases}\tag{6}$$

where the recurrence formulae for $\varphi_n(z)$ and $\omega_n(z)$respectively are

$$\phi_n(z)=\begin{cases}(1+\Lambda_{21})\phi_0(z)\ n=1\\ \Pi_{12}\begin{bmatrix}\Lambda_{32}\phi_{n-1}(z+2it)\\ -2it\Pi_{32}\omega_{n-1}'(z+2it)\\ -4t^2\Pi_{32}\phi_{n-1}"(z+2it)\end{bmatrix}\ n=2,3,4,...\end{cases}\tag{7}$$

$$\omega_n(z)=\begin{cases}(1+\Pi_{21})\omega_0(z)\ n=1\\ \Pi_{32}\Lambda_{12}\begin{bmatrix}\omega_{n-1}(z+2it)\\ -2it\phi_{n-1}'(z+2it)\end{bmatrix}\ n=2,3,4,...\end{cases}\tag{8}$$

In which the homogeneous solution for an edge dislocation in region S_1 is

$$\begin{cases}\phi_0(z)=Q\log(z-z_t)\\ \omega_0(z)=\frac{Q(z-\overline{z_t})}{z-z_t}+\overline{Q}\log(z-z_t)\end{cases}\tag{9}$$

$$Q=\frac{G_1(b_x+ib_y)}{i\pi(\kappa_1+1)}\tag{10}$$

where b_x+ib_y is an edge dislocation and z_t indicate the location of the edge dislocation in region S_1. Note that the corresponding homogeneous solution can be obtained if one lets $\Pi_{kj}=\Lambda_{kj}=0$ in Eqs. (5) and (6).

2.2 Edge rislocation in region S_2

The complete complex potential solution for an edge dislocation in region S_2 of the tri-material as shown in Fig. 2(b) is

$$\phi(z)=\begin{cases}(1+\Lambda_{32})\sum\limits_{n=1}^{\infty}\phi_n(z) & z\in S_3\\ \phi_0(z)+\Pi_{12}\overline{\omega_0}(z)+\sum\limits_{n=1}^{\infty}\phi_{n+1}(z)+\Lambda_{12}^{-1}\sum\limits_{n=1}^{\infty}\overline{\omega_{n+1}}(z) & z\in S_2\\ (1+\Lambda_{12})\phi_0(z)+\left(1+\Lambda_{12}^{-1}\right)\sum\limits_{n=1}^{\infty}\overline{\omega_{n+1}}(z) & z\in S_1\end{cases} \tag{11}$$

$$\omega(z)=\begin{cases}(1+\Pi_{32})\sum\limits_{n=1}^{\infty}\omega_n(z)+2it(\Lambda_{32}-\Pi_{32})\sum\limits_{n=1}^{\infty}\phi_n'(z) & z\in S_3\\ \omega_0(z)+\Lambda_{12}\overline{\phi_0}(z)+\sum\limits_{n=1}^{\infty}\omega_{n+1}(z)+\Pi_{12}^{-1}\sum\limits_{n=1}^{\infty}\overline{\phi_{n+1}}(z) & z\in S_2\\ (1+\Pi_{12})\omega_0(z)+\left(1+\Pi_{12}^{-1}\right)\sum\limits_{n=1}^{\infty}\overline{\phi_{n+1}}(z) & z\in S_1\end{cases} \tag{12}$$

where the recurrence formulae for $\varphi_n(z)$ and $\omega_n(z)$ respectively are

$$\phi_n(z)=\begin{cases}\phi_0(z)+\Pi_{12}\overline{\omega_0}(z) & n=1\\ \Pi_{12}\begin{bmatrix}\Lambda_{32}\phi_{n-1}(z+2it)\\ -2it\Pi_{32}\omega_{n-1}'(z+2it)\\ -4t^2\Pi_{32}\phi_{n-1}"(z+2it)\end{bmatrix} & n=2,3,4,...\end{cases} \tag{13}$$

$$\omega_n(z)=\begin{cases}\omega_0(z)+\Lambda_{12}\overline{\phi_0}(z) & n=1\\ \Pi_{32}\Lambda_{12}\begin{bmatrix}\omega_{n-1}(z+2it)\\ -2it\phi_{n-1}'(z+2it)\end{bmatrix} & n=2,3,4,...\end{cases} \tag{14}$$

in which the homogeneous solution for an edge dislocation in region S_2 is

$$\begin{cases}\phi_0(z)=Q\log(z-z_t)\\ \omega_0(z)=\frac{Q(z-\overline{z_t})}{z-z_t}+\overline{Q}\log(z-z_t)\end{cases} \tag{15}$$

$$Q=\frac{G_2(b_x+ib_y)}{i\pi(\kappa_2+1)} \tag{16}$$

where b_x + ib_y is an edge dislocation and z_t indicate the location of the edge dislocation in region S_2. Note that the corresponding homogeneous solution can be obtained if one lets $\Pi_{kj}=\Lambda_{kj}=0$ in Eqs. (11) and (12).

3 Crack modeling

In order to solve the crack problem, we consider a single traction-free crack $2a$ to be situated in the infinite plane under a remote uniform tensile load. It is assumed that the distributed edge dislocation with the density $b(s) = b_x(s)+\mathrm{i}b_y(s)$ is placed along the prospective crack segment in an infinite plane. The appropriate complex potentials for a crack in homogeneous medium will take the following form:

$$\begin{cases} \phi_0(z) = \int\limits_{2a} Q(s)\log(z-z_t)\,ds \\ \omega_0(z) = \int\limits_{2a} \frac{Q(s)(z-\overline{z_t})}{z-z_t}ds + \int\limits_{2a} \overline{Q(s)}\log(z-z_t)\,ds \end{cases} \tag{17}$$

where

$$Q(s) = \frac{G_j\left(b_x(s)+ib_y(s)\right)}{i\pi(\kappa_j+1)} \quad j=1,2 \tag{18}$$

Meanwhile, the solution for a homogeneous infinite plate subjected to a remote uniform tensile σ_x. acting with an angle β to the x-axis can be trivially given as

$$\begin{cases} \phi_0(z) = \frac{\sigma_x}{4}z \\ \omega_0(z) = \frac{\sigma_x}{4}z - \frac{\sigma_x e^{-2i\beta}}{2}z \end{cases} \tag{19}$$

Due to the traction-free condition along the crack surface, the total resultant force across the crack surface must be balanced by the given resultant force across the crack segment in the unflawed media. This results in

$$\left\{\phi(z)+\overline{\omega(z)}+(z-\bar{z})\overline{\phi'(z)}\right\}_{crack} = -Y(z_0)+iX(z_0) \tag{20}$$

3.1 Crack modeling in region S_1

Let a crack be located in region S_1 of plane layered tri-material media. The corresponding complex potentials are given by substituting Eq. (17) into Eqs. (5) and (6) for $z \in S_1$, respectively such as

$$\begin{aligned} \phi_1(z) = &\int\limits_{2a} Q(s)\log(z-z_t)\,ds + \Pi_{21}\int\limits_{2a}\frac{\overline{Q(s)}(z-z_t)}{z-\overline{z_t}}ds \\ &+\Pi_{21}\int\limits_{2a} Q(s)\log(z-\overline{z_t})\,ds + \int\limits_{2a}\left(1+\Lambda_{12}^{-1}\right)\sum_{\mathrm{n}=1}^{\infty}\overline{\omega_{n+1}}(z)ds \end{aligned} \tag{21}$$

and

$$\begin{aligned} \omega_1(z) = &\int\limits_{2a} \frac{Q(s)(z-\overline{z_t})}{z-z_t}ds + \int\limits_{2a}\overline{Q(s)}\log(z-z_t)\,ds \\ &+\Lambda_{21}\int\limits_{2a}\overline{Q(s)}\log(z-\overline{z_t})\,ds + \int\limits_{2a}\left(1+\Pi_{12}^{-1}\right)\sum_{\mathrm{n}=1}^{\infty}\overline{\phi_{n+1}}(z)ds \end{aligned} \tag{22}$$

The resultant force across the crack surface for the region S_1 can be written by substituting two complex solutions $\varphi_1(z)$ and $\omega_1(z)$ from Eqs. (21) and (22) into Eq. (20). Applications of principle of superposition lead to the integral equation with logarithmic singular Kernels as

$$\int_{2a} L_1(z_0,\overline{z_0},z_t,\overline{z_t})Q(s)ds+\int_{2a} L_2(z_0,\overline{z_0},z_t,\overline{z_t})\overline{Q(s)}ds+C_1+iC_2=-Y(z_0)+iX(z_0) \tag{23}$$

where

$$L_1(z_0,\overline{z_0},z_t,\overline{z_t})=H_1(z_0,\overline{z_0},z_t,\overline{z_t})+B_1(z_0,\overline{z_0},z_t,\overline{z_t})+T_1(z_0,\overline{z_0},z_t,\overline{z_t}) \tag{24}$$

$$L_2(z_0,\overline{z_0},z_t,\overline{z_t})=H_2(z_0,\overline{z_0},z_t,\overline{z_t})+B_2(z_0,\overline{z_0},z_t,\overline{z_t})+T_2(z_0,\overline{z_0},z_t,\overline{z_t}) \tag{25}$$

in which H_1 and H_2 are homogeneous solutions expressed as

$$H_1(z_0,\overline{z_0},z_t,\overline{z_t})=2\log|z-z_t| \tag{26}$$

$$H_2(z_0,\overline{z_0},z_t,\overline{z_t})=\frac{(z-z_t)}{\overline{z}-\overline{z_t}} \tag{27}$$

while B_1 and B_2 are complimentary solutions of bi-material problems expressed as

$$B_1(z_0,\overline{z_0},z_t,\overline{z_t})=\Pi_{21}\log(z-\overline{z_t})+\Lambda_{21}\log(\overline{z}-z_t)+\Pi_{21}\frac{(z-\overline{z})(\overline{z_t}-z_t)}{(\overline{z}-z_t)^2} \tag{28}$$

$$B_2(z_0,\overline{z_0},z_t,\overline{z_t})=\Pi_{21}\frac{(z-z_t)}{(z-\overline{z_t})}+\Pi_{21}\frac{(z-\overline{z})}{(\overline{z}-z_t)} \tag{29}$$

$T_1(z_0,\overline{z_0},z_t,\overline{z_t})$ and $T_2(z_0,\overline{z_0},z_t,\overline{z_t})$ are the series functions with the coefficients $Q(s)$ and $\overline{\mathrm{Q(s)}}$for crack located in regionS_1.

Meanwhile, the resultant force corresponding to the unflawed media can be obtained by substituting the homogeneous solution from Eq. (19) into Eq. (1) as

$$-Y(z_0)+iX(z_0)=\frac{\sigma_x}{2}z-\frac{\sigma_x}{2}\bar{z} \tag{30}$$

In addition, the single-valued condition of the dislocation density must be satisfied, i.e.

$$\int_{2a}[b_x(s)+ib_y(s)]ds=0 \tag{31}$$

Clearly, the dislocation density function can be found by separating Eq. (23) into real and imaginary parts, respectively as

$$\begin{aligned}&\int_{2a} Re\left[L_1(z_0,\overline{z_0},z_t,\overline{z_t})+L_2(z_0,\overline{z_0},z_t,\overline{z_t})\right]b_x(s)ds\\&+\int_{2a} Im\left[-L_1(z_0,\overline{z_0},z_t,\overline{z_t})+L_2(z_0,\overline{z_0},z_t,\overline{z_t})\right]b_y(s)ds+C_1=-Y(z_0)\end{aligned} \tag{32}$$

and

$$\begin{aligned}&\int_{2a} Im\left[L_1(z_0,\overline{z_0},z_t,\overline{z_t})+L_2(z_0,\overline{z_0},z_t,\overline{z_t})\right]b_x(s)ds\\&+\int_{2a} Re\left[L_1(z_0,\overline{z_0},z_t,\overline{z_t})-L_2(z_0,\overline{z_0},z_t,\overline{z_t})\right]b_y(s)ds+C_2=X(z_0)\end{aligned} \tag{33}$$

Eqs. (32) and (33) together with the subsidiary condition Eq. (31) will be solved numerically by the boundary element technique where a crack was divided by N line segments as indicated in Fig. 3. In the calculation, the linear interpolation formulae with undetermined coefficients are applied to approximate the dislocation distribution along the elements, except at vicinity of crack tip where the dislocation distribution preserves a square-root singularity. The interpolation formulae in local coordinate's s_j *(1* $\leq j \leq$ *N)* are defined as

$$b_i(s_1)=b_{i,1}\left(\sqrt{\frac{2d_1}{d_1+s_1}}-1\right)+b_{i,2} \qquad \text{for the left tip} \tag{34}$$

$$b_i(s_N)=b_{i,N+1}\left(\sqrt{\frac{2d_N}{d_N-s_N}}-1\right)+b_{i,N} \qquad \text{for the right tip} \tag{35}$$

$$b_i(s_j)=b_{i,j}\frac{d_j-s_j}{2d_j}+b_{i,j+1}\frac{d_j+s_j}{2d_j} \qquad \text{for intermediate segments} \tag{36}$$

where (i = 1, 2), d_j *(1* $\leq j \leq$ *N)* are the half length of each line segment, and $b_{i,j}$ *(1* $\leq j \leq$ *N+1)* are the unknown coefficients. Note that the singular integral equations derived in this paper contain the logarithmic functions which are multi-valued functions in complex variable domain. Suitable branch cuts are designed to have the principal value of θ_p such as $0 \leq \theta_p < 2\pi$ where the cut is introduced along the ray extending from the crack tip (or branch point) to infinity. In these cut structures, it is verified that the discontinuity of displacements across the brunch cut can be avoided.

After using the interpolation formulae, the logarithmic integration presented in Eq. (23) can be evaluated exactly for some conditions. Otherwise, the following Gauss-

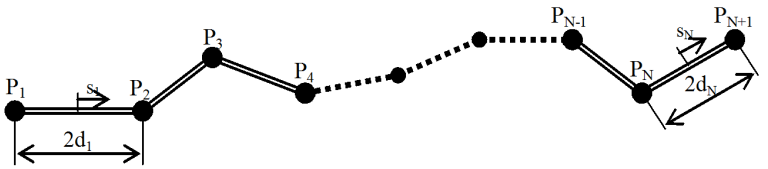

Figure 3: Division and nodal distribution of a crack.

Chebyshev integration rule is needed.

$$\int_{-d}^{d} G(s)ds = \frac{\pi d}{M}\sum_{m=1}^{M} G(s_m)\sin\left(\frac{2m-1}{2M}\pi\right) \text{ with } s_m = d\cos\left(\tfrac{2m-1}{2M}\pi\right) \tag{37}$$

m = 1, 2, …., M

The system of $2N+2$ simultaneous algebraic equations have been solved for the undetermined dislocation coefficients $b_{i,j}$, then the mode-I and mode-II stress intensity factors can be obtained as

$$K_A = K_{1A} - iK_{2A} = -e^{-i\alpha}(2\pi)^{\frac{3}{2}}\lim_{s\to 0}\sqrt{s}\mu(s) = -(2\pi)^{\frac{3}{2}}(2d)^{1/2}e^{-i\alpha}(b_{1,1}+ib_{2,1}) \tag{38}$$

$$\begin{aligned} K_B = K_{1B} - iK_{2B} &= e^{-i\alpha}(2\pi)^{\frac{3}{2}}\lim_{s\to l}\sqrt{(l-s)}\mu(s) \\ &= (2\pi)^{\frac{3}{2}}(2d)^{1/2}e^{-i\alpha}(b_{1,N+1}+ib_{2,N+1}) \end{aligned} \tag{39}$$

3.2 Crack modeling in region S_2

Let a crack be located in region S_2 of plane layered tri-material media. The corresponding complex potentials are given by substituting Eq. (17) into Eqs. (11) and (12) for $z \in S_2$, respectively as

$$\begin{aligned} \phi_1(z) = &\int_{2a} Q(s)\log(z-z_t)\,ds + \Pi_{12}\int_{2a}\frac{\overline{Q(s)}(z-z_t)}{z-\overline{z_t}}ds \\ &+\Pi_{12}\int_{2a} Q(s)\log(z-\overline{z_t})\,ds + \int_{2a}\left(\sum_{n=1}^{\infty}\phi_{n+1}(z) + \Lambda_{12}^{-1}\sum_{n=1}^{\infty}\overline{\omega_{n+1}}(z)\right)ds \end{aligned} \tag{40}$$

and

$$\omega_1(z) = \int_{2a} \frac{Q(s)(z-\overline{z_t})}{z-z_t} ds + \int_{2a} \overline{Q(s)} \log(z-z_t)\, ds + \Lambda_{12} \int_{2a} \overline{Q(s)} \log(z-\overline{z_t})\, ds + \int_{2a} \left(\sum_{n=1}^{\infty} \omega_{n+1}(z) + \Pi_{12}^{-1} \sum_{n=1}^{\infty} \overline{\phi_{n+1}}(z) \right) ds \tag{41}$$

The resultant force across the crack surface for the region S_2 can be written by substituting two complex solutions $\varphi_2(z)$ and $\omega_2(z)$ from Eqs. (40) and (41) into Eq. (20). Applications of principle of superposition lead to the integral equation with logarithmic singular Kernels such as

$$\int_{2a} L_1(z_0, \overline{z_0}, z_t, \overline{z_t}) Q(s) ds + \int_{2a} L_2(z_0, \overline{z_0}, z_t, \overline{z_t}) \overline{Q(s)} ds + C_1 + iC_2 = -Y(z_0) + iX(z_0) \tag{42}$$

where

$$L_1(z_0, \overline{z_0}, z_t, \overline{z_t}) = H_1(z_0, \overline{z_0}, z_t, \overline{z_t}) + B_1(z_0, \overline{z_0}, z_t, \overline{z_t}) + S_1(z_0, \overline{z_0}, z_t, \overline{z_t}) \tag{43}$$

$$L_2(z_0, \overline{z_0}, z_t, \overline{z_t}) = H_2(z_0, \overline{z_0}, z_t, \overline{z_t}) + B_2(z_0, \overline{z_0}, z_t, \overline{z_t}) + S_2(z_0, \overline{z_0}, z_t, \overline{z_t}) \tag{44}$$

in which H_1 and H_2 are homogeneous solutions expressed as

$$H_1(z_0, \overline{z_0}, z_t, \overline{z_t}) = 2\log|z - z_t| \tag{45}$$

$$H_2(z_0, \overline{z_0}, z_t, \overline{z_t}) = \frac{(z-z_t)}{\overline{z}-\overline{z_t}} \tag{46}$$

while B_1 and B_2 are complimentary solutions expressed as

$$B_1(z_0, \overline{z_0}, z_t, \overline{z_t}) = \Pi_{12} \log(z-\overline{z_t}) + \Lambda_{12} \log(\overline{z}-z_t) + \Pi_{12} \frac{(z-\overline{z})(\overline{z_t}-z_t)}{(\overline{z}-z_t)^2} \tag{47}$$

$$B_2(z_0, \overline{z_0}, z_t, \overline{z_t}) = \Pi_{12} \frac{(z-z_t)}{(z-\overline{z_t})} + \Pi_{12} \frac{(z-\overline{z})}{(\overline{z}-z_t)} \tag{48}$$

and $T_1(z_0, \overline{z_0}, z_t, \overline{z_t})$ and $T_2(z_0, \overline{z_0}, z_t, \overline{z_t})$ are the series functions with the coefficients $Q(s)$ and $\overline{\mathrm{Q(s)}}$for crack located in region S_2.

Using the similar procedures as section 3.1, the stress intensity factors can also be obtained from Eqs. (38) and (39).

4 Numerical results

Bi-material problem with a crack is considered first to examine the accuracy of the present approach (see Fig. 4). The normalized stress intensity factors obtained by the present method are given in Tables 1 and 2, together with those valued obtained in [Cook (1972); Tada (1973)]. It can be seen from both tables that the present approach provides reliable results compare with published values. Fig. 5 indicates more clearly that the calculated values of the normalized stress intensity factors yield a good accuracy if the number of line segments N = 60.

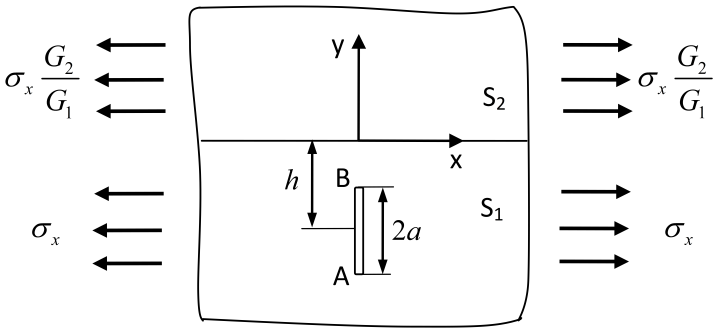

Figure 4: A crack perpendicular to the bi-material

Table 1: Comparison between the calculated and published values of K_I at tip-B in Fig. 4 for elastic half-plane

$G_2/G_1=0$							
h/a	Cook (1972)	N=30	N=60	a/h	Tada (1973)	N=30	N=60
1.01	3.72	3.920002	3.856978				
1.05	2.159	2.237421	2.195138	0.3	1.033	1.040684	1.035802
1.1	1.759	1.802039	1.78092	0.4	1.052	1.066778	1.061675
1.15	1.575	1.607071	1.592698	0.5	1.094	1.106251	1.100771
1.2	1.464	1.490582	1.479207	0.6	1.148	1.165406	1.159289
1.25	1.388	1.411402	1.401669	0.7	1.243	1.256783	1.249529
1.5	1.204	1.221511	1.214724	0.8	1.385	1.411382	1.401646
2	1.091	1.106309	1.100834	0.9	1.688	1.747617	1.728598
5	1.011	1.024491	1.019738				
10	1.003	1.01574	1.011043				

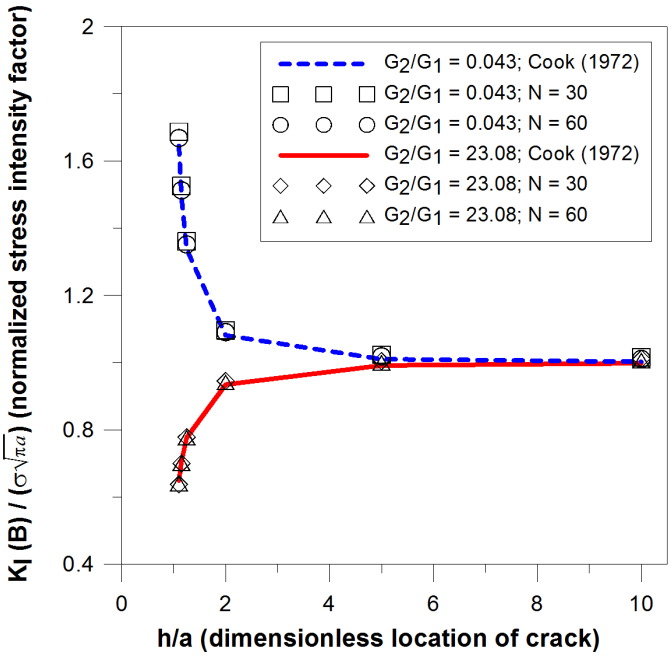

Figure 5: Comparison between the calculated and published values of normalized mode-I stress intensity factors at tip-B versus dimensionless location of a crack perpendicular to the bi-material.

Note that all these stress intensity factors presented here are obtained by summation of series solution up to the first six terms, since they are checked to achieve a good approximation for most combination materials. Table 3 shows that the contributions of the stress intensity factors for leading terms of the series when G_2/G_1 = *0.5,* G_3/G_1 = *2, a/t = 0.1*. It is likely to see that the leading six terms make over 99% contribution, making the series solution rapidly convergent. This demonstrates the accuracy and the efficiency of the proposed method.

Figs. 6 and 7 show the variation of normalized mode-I stress intensity factor at tip-B versus dimensionless location of a crack h/a in region S_1 with different G_2/G_1. In this example, $G_3/G_1 = 1$, $\upsilon_1 = \upsilon_2 = \upsilon_3 = 0.3$, and *a/t = 0.1* are used. It is seen from Fig. 4 that the softer materials may always give enhancement effect on stress intensity factors when a crack approaching interface L. On the other hand, from Fig. 7 shows that the softer materials may always give retardation effect on stress intensity factors when a crack approaching interfaces L. It is indicated that the nearest material property from crack tip has more dominant effects on the variation of stress intensity factor of a crack in straight multi layer plane. The calculated

Table 2: Comparison between the calculated and published values of K_I at tip-B in Fig. 4 for bi-material

h/a	G_2/G_1=0.043			G_2/G_1=23.08		
	Cook (1972)	N=30	N=60	Cook (1972)	N=30	N=60
1.1	1.6451	1.68641	1.667741	0.6486	0.637307	0.640086
1.15	1.4942	1.525352	1.512304	0.7046	0.699704	0.700413
1.25	1.3369	1.360383	1.351276	0.7764	0.777834	0.776529
2	1.0808	1.095836	1.090448	0.9344	0.945198	0.941136
5	1.01	1.023262	1.018517	0.9912	1.004103	0.999476
10	1.0023	1.015454	1.010759	0.9979	1.010942	1.006271

Table 3: Contribution of the leading terms n = 2-6 for $K_I$at tip-B in Fig. 1(a)

Terms	Contribution(%)
2	83.46
3	13.49
4	2.41
5	0.45
6	0.09

results with $h/a = 2$, $G_2/G_1 = 0.3$, $G_3/G_1 = 1$, $a/t = 0.1$, $\nu_1 = \nu_2 = \nu_3 = 0.3$ shown in Fig. 6 are also compared to those using FEM with error less than 1% which demonstrates the accuracy and efficiency used in this approach.

Figs. 8-9 show the variation of normalized mode-I and mod-II stress intensity factors at tip-B versus an inclined angle of a crack with different G_3/G_1. In this example, $\upsilon_1 = \upsilon_2 = \upsilon_3 = 0.3$, *h/a = 1.3,* and *a/t = 0.1* are used. It is clearly seen that mode-I and mode-II stress intensity factors at tip-B may always have similar values and trends for fixed value of G_2/G_1, even though the material properties G_3/G_1 is vary. It can be concluded that the material property in region S_2 has more dominant effects than material property in region $S_3$to the mode-I and mode-II stress intensity factors of a crack located in region S_1.

The results of the variation of normalized mode-I stress intensity factor in crack tip versus dimensionless location of a crack h/a in region S_2 with different G_3/G_2 are displayed in Figs 10-13. In this example, $\upsilon_1 = \upsilon_2 = \upsilon_3 = 0.3$, and *a/t = 0.1* are used. It is obviously seen from Fig. 10 with $G_1/G_2 = 0.7$ that the softer material may always give enhancement effect on the stress intensity factors at tip-A when a crack approaching interface L. Meanwhile from Fig. 11 with $G_1/G_2 = 2$ shown

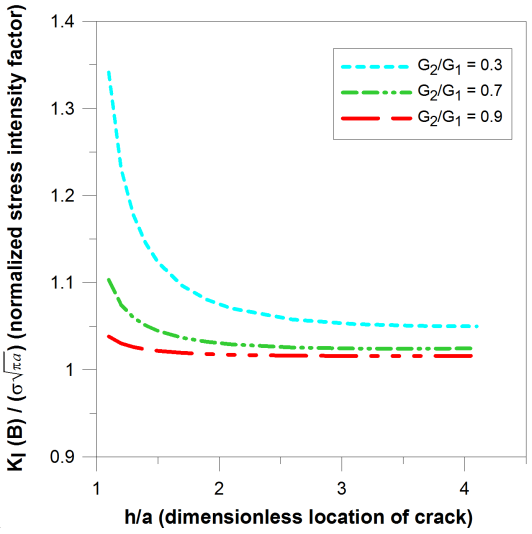

Figure 6: Normalized mode-I stress intensity factors versus dimensionless location of crack located in region S_1 with different softer material G_2/G_1 for $G_3/G_1 = 1$, $\upsilon_1 = \upsilon_2 = \upsilon_3 = 0.3$, and *a/t = 0.1*.

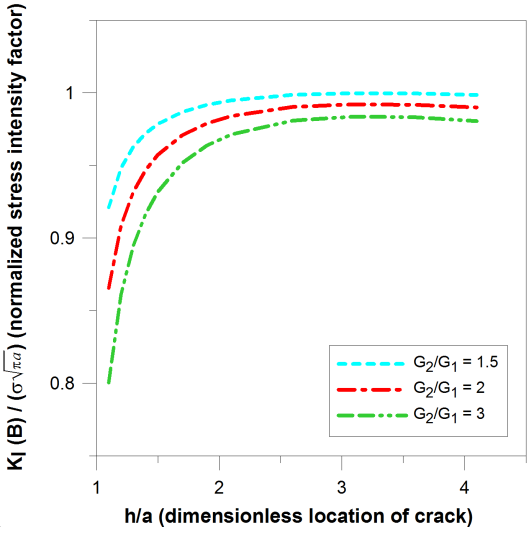

Figure 7: Normalized mode-I stress intensity factors versus dimensionless location of crack located in region S_1 with different stiffer material G_2/G_1 for $G_3/G_1 = 1$, $\upsilon_1 = \upsilon_2 = \upsilon_3 = 0.3$, and *a/t = 0.1*.

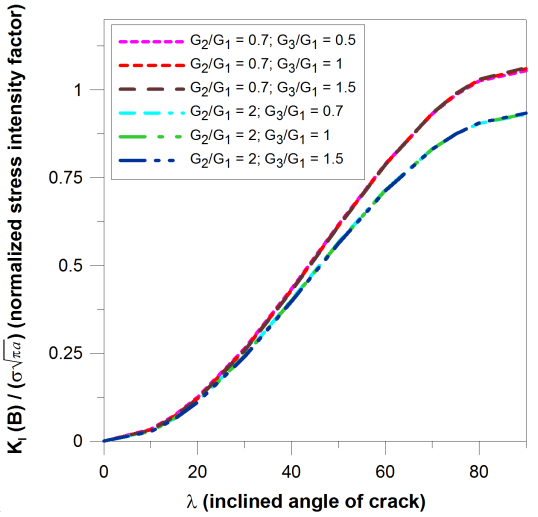

Figure 8: Normalized mode-I stress intensity factors versus inclined angle of crack located in region S_1 with different material G_3/G_1 for $G_2/G_1 = 0.7$or $G_2/G_1 = 2$, $\upsilon_1 = \upsilon_2 = \upsilon_3 = 0.3$, *h/a = 1.3,* and *a/t = 0.1.*

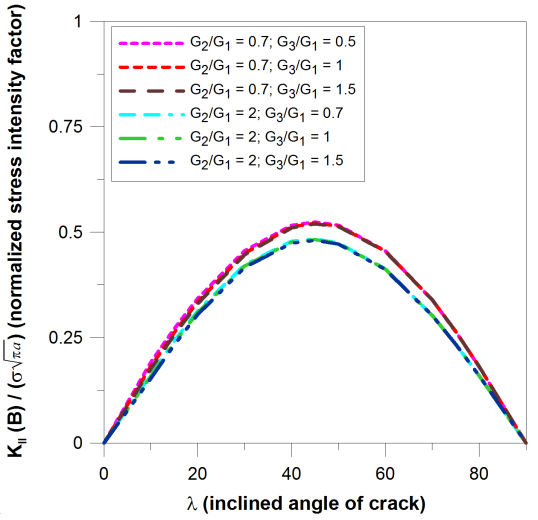

Figure 9: Normalized mode-II stress intensity factors versus inclined angle of crack located in region S_1 with different material G_3/G_1 for $G_2/G_1 = 0.7$ or $G_2/G_1 = 2$, $\upsilon_1 = \upsilon_2 = \upsilon_3 = 0.3$, *h/a = 1.3,* and *a/t = 0.1.*

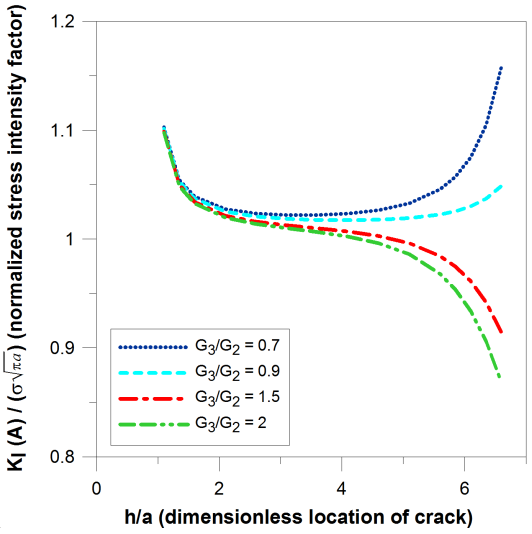

Figure 10: Normalized mode-I stress intensity factors at tip-A versus dimensionless location of crack located in region S_2 with different material G_3/G_2 for $G_1/G_2 = 0.7$, $\upsilon_1 = \upsilon_2 = \upsilon_3 = 0.3$, and *a/t = 0.1*.

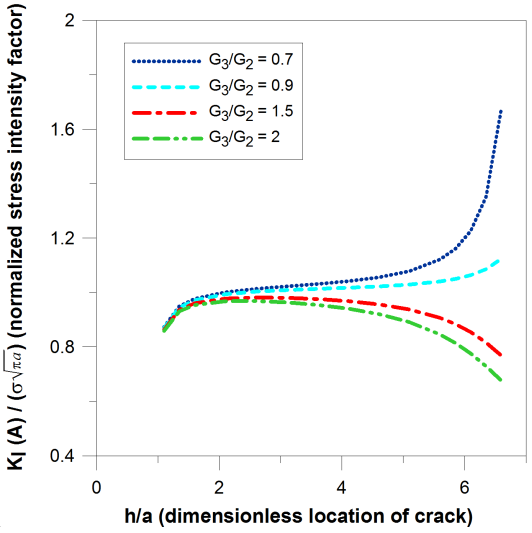

Figure 11: Normalized mode-I stress intensity factors at tip-A versus dimensionless location of crack located in region S_2 with different material G_3/G_2 for $G_1/G_2 = 2$, $\upsilon_1 = \upsilon_2 = \upsilon_3 = 0.3$, and *a/t = 0.1*.

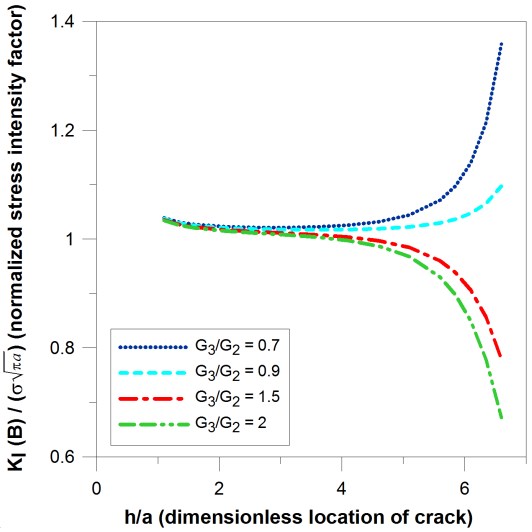

Figure 12: Normalized mode-I stress intensity factors at tip-B versus dimensionless location of crack located in region S_2 with different material G_3/G_2 for $G_1/G_2 = 0.7$, $\upsilon_1 = \upsilon_2 = \upsilon_3 = 0.3$, and *a/t = 0.1*.

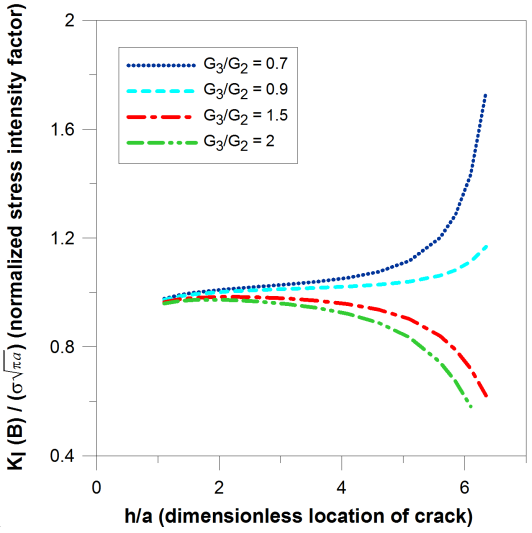

Figure 13: Normalized mode-I stress intensity factors at tip-B versus dimensionless location of crack located in region S_2 with different material G_3/G_2 for $G_1/G_2 = 2$, $\upsilon_1 = \upsilon_2 = \upsilon_3 = 0.3$, and *a/t = 0.1*.

that the stiffer material may always give retardation effect on the stress intensity factors at tip-A when a crack approaching interface L. On the other hand, both in Figs. 8 and 9 shows that when a crack approaching interface $L*$, the stress intensity factors at tip-A may always increase for material S_2 is stiffer than material S_1 and may always decrease for material S_2 is softer than material S_3.

Moreover, from Figs. 12-13 shown that the material combinations of G_1/G_2 may give less effects on the stress intensity factors at tip-B for a crack located near interface L. Nevertheless, the material combinations of G_3/G_2may always give more effects on stress intensity factor at tip-B as well as on stress intensity factor at tip-A when a crack approaching interface $L*$.

5 Conclusions

A solution of a crack interacting with a tri-material composite under a remote uniform tensile load is presented in this paper. The solution is based on Muskhelishvili complex potential in conjunction with logarithmic singular integral equation approach. Some numerical calculations are performed to investigate the effect of material properties combinations on mode-I and mode-II stress intensity factors. We conclude that the stress intensity factors may always decrease when a crack approaching the stiffer material. On the other hand, the stress intensity factors may always increase when a crack approaching the softer material.

References

Chao, C.K.; Chen, F.M. (2004): Thermal stresses in an isotropic trimaterial interacted with a pair of point heat source and heat sink. *International Journal of Solids and Stuctures*, vol. 41, pp. 6233-6247.

Chao, C.K.; Kao, B. (1997): A thin cracked layer bonded to an elastic half-space under an antiplane concentrated load. *International Journal Fracture*, vol. 83, no. 3, pp. 223-241.

Chao, C. K.; Lee, J. Y. (1996): Interaction between a crack and a circular elastic inclusion under remote uniform heat flow. *International Journal of Solids and Structures*, vol. 33, pp. 3865-3880.

Chao, C. K.; Shen, M. H. (1995): Solutions of thermoelastic crack problems in bonded dissimilar media or half-plane medium. *International Journal of Solids and Structures*, vol. 32, pp. 3537-3554.

Chao, C.K.; Young, C.W. (1998): Antiplane interaction of a crack with a circular inclusion in an elastic half plane. *Journal of Engineering Mechanics*, vol. 124, no. 2, pp. 167-175.

Chao, C. K.; Wikarta, A. (2012): Mode-III stress intensity factors of a three-phase composite with an eccentric circular inclusion. *CMES: Computer Modeling in Engineering & Sciences* vol. 84, no.5, pp. 439-458.

Chao, C. K.; Wikarta, A.; Korsunsky, A. M. (2010): Anti-plane interaction of a crack and reinforced elliptic hole in an infinite matrix. *Theoretical and Applied Fracture Mechanics*, vol. 53, pp. 205-210.

Chen, Y.Z. (1992): Stress intensity factors for curved circular crack in bonded dissimilar materials. *Theoretical and Applied Fracture Mechanics*, vol. 17, pp. 189-196.

Chen, Y. Z.; Chen, R. S. (1997): Interaction between curved crack and elastic inclusion in an infinite plate. *Archive of Applied Mechanics*, vol. 67, pp. 566-575.

Chen, Y. Z.; Cheung, Y. K. (1990): New integral equation approach for the crack problem in elastic half-plane. *International Journal of Fracture*, vol. 46, pp. 57-69.

Choi, S.T.; Earmme Y.Y. (2002): Elastic study on singularities interacting with interfaces using alternating technique: part II. isotropic trimaterial. *International Journal of Solids and Structures*, vol. 39, no. 5, pp. 1199-1211.

Cook, T. S.; Erdogan, F. (1972): Stresses in bonded materials with a crack perpendicular to the interface. *International Journal of Engineering Science*, vol. 10, no.8, pp. 677-697.

Tada, H.; Paris, P.C.; Irwin, G.R. (1973): *The Stress Analysis of Cracks Handbook, 1st edition*, Del Research Corporation, Hellertown, Pennsylvania.